Complex Diffusion Processes for Image Filtering

Guy Gilboa[1], Yehoshua Y. Zeevi[1], and Nir A. Sochen[2]

[1] Department of Electrical Engineering, Technion - Israel Institute of Technology
Technion City, Haifa 32000, ISRAEL
gilboa@tx.technion.ac.il, zeevi@ee.technion.ac.il
[2] Department of Applied Mathematics, University of Tel-Aviv Ramat-Aviv, Tel-Aviv 69978, Israel sochen@math.tau.ac.il

Abstract. *This paper is concerned with the search for a general framework that naturally unifies smoothing and enhancement processes. We present a generalization of linear and nonlinear scale space in the complex domain, by combining the diffusion equation with the simplified schrodinger equation. A fundamental solution for the linear complex case is developed. A preliminary analysis of the complex diffusion is made, showing that the generalized diffusion has properties of both forward and inverse diffusion. An important observation, supported theoretically and numerically, is that the imaginary part can be regarded as an edge detector (smoothed second derivative) after rescaling by time, when the complex diffusion coefficient approaches the real axis. Based on this observation, a nonlinear complex process for ramp preserving denoising is developed.*

Keywords: *scale-space, image filtering, image denoising , image enhancement, nonlinear diffusion, complex diffusion.*

1 Introduction

The scale-space approach is by now a well established multi-resolution technique for image structure analysis (see [5],[1],[4]). Originally, the Gaussian representation introduced a scale dimension by convolving the original image with a Gaussian of a standard deviation $\sigma = \sqrt{2t}$. This is analogous to solving the linear diffusion equation

$$I_t = c\nabla^2 I, \quad I|_{t=0} = I_0, \quad 0 < c \in \mathbb{R}, \tag{1}$$

with a constant diffusion coefficient $c = 1$.

Perona and Malik (P-M) [3] proposed a nonlinear adaptive diffusion process, where diffusion takes place with a variable diffusion coefficient in order to reduce the smoothing effect near edges. The P-M nonlinear diffusion equation is of the form:

$$I_t = \nabla \cdot (c(|\nabla I|)\nabla I), \qquad c(\cdot) > 0 \tag{2}$$

where c is a decreasing function of the gradient.

Our aim is to see if the linear and nonlinear scale-spaces can be viewed as special cases of a more general theory of complex diffusion-type processes.

Complex diffusion-type processes are encountered i.e. in quantum physics and in electro-optics. Let us briefly review these flows. Note that although these flows have a diffusion structure, because of the complex coefficient, they retain wave propagation properties.

The time dependent *Schrödinger equation* is the fundamental equation of quantum mechanics. In the simplest case for a particle without spin in an external field it has the form

$$i\hbar\frac{\partial\psi}{\partial t} = -\frac{\hbar^2}{2m}\Delta\psi + V(x)\psi \quad , \tag{3}$$

where $\psi = \psi(t,x)$ is the wave function of a quantum particle, m is the mass of the particle, $\hbar$ is Planck's constant, $V(x)$ is the external field potential, Δ is the Laplacian and $i \doteq \sqrt{-1}$. With an initial condition

$$\psi|_{t=0} = \psi_0(x) \quad ,$$

requiring that $\psi(t,\cdot) \in L_2$ for each fixed t, the solution is

$$\psi(t,\cdot) = e^{-\frac{i}{\hbar}tH}\psi_0 \quad , \tag{4}$$

where the exponent is a shorthand for the corresponding power series, and the higher order terms are defined recursively by $H^n\Psi = H(H^{n-1}\Psi)$. The operator

$$H = -\frac{\hbar^2}{2m}\Delta + V(x), \tag{5}$$

called the *Schrödinger operator*, is interpreted as the energy operator of the particle under consideration. The first term is the kinetic energy and the second is the potential energy. The duality relations that exist between the Schrödinger equation and diffusion theory have been studied elsewhere [2]. Another important complex partial differential equation is the *complex Ginzburg-Landau equation* (CGL). It is a nonlinear complex diffusion-type equation related to amplitude of traveling wave systems. It appears in the theory of phase transitions and instability waves, having the (1D, lowest order case) form of

$$u_t = (1+i\nu)u_{xx} + Ru - (1+i\mu)|u|^2u \quad , \tag{6}$$

where $u(x,t)$ is a complex amplitude envelope, R a finite wave length instability measure, and ν and μ are strength measures of the linear and nonlinear dispersions, respectively.

In both cases a non-linearity is introduced by adding a potential term while the kinetic energy stays linear. In this study we employ the equation with zero potential (no external field) but with non-linear "kinetic energy". To better understand the complex flow, we study in Section 2 the linear case and derive the fundamental solution. We show that for small imaginary part the flow is approximately a linear real diffusion for the real part while the imaginary part behaves

like a second derivative of the real part. Indeed as expected, the imaginary part is directly related to the localized phase and zero crossings of the image, and this is one of the important properties obtained by generalizing the diffusion approach to the complex case. The non-linear case is studied in Section 3 and the intuition gained from the linear case is used in order to construct a special non-linear complex diffusion scheme which preserves ramps. The advantage over higher order PDE's and over the P-M algorithm is demonstrated in one- and two-dimensional examples.

2 Linear Complex Diffusion

2.1 Problem Definition

We consider the following initial value problem:

$$\begin{aligned} I_t &= cI_{xx}, \qquad t>0, \qquad x\in\mathbb{R} \\ I(x;0) &= I_0\in\mathbb{R}, \quad c, I\in\mathbb{C}. \end{aligned} \tag{7}$$

This equation is a generalization of two equations: the linear *diffusion* equation (1) for $c\in\mathbb{R}$ and the simplified *Shcrödinger* equation, i.e. $c\in\mathbb{I}$ and $V(x)\equiv 0$. When $c\in\mathbb{R}$ there are two cases: for $c>0$ the process is a well posed forward diffusion, whereas for $c<0$ an ill posed unstable inverse diffusion process is obtained.

2.2 Fundamental Solution

We seek the complex fundamental solution $h(x;t)$ that satisfies the relation:

$$I(x;t) = I_0 * h(x;t) \tag{8}$$

where $*$ denotes convolution. We rewrite the complex diffusion coefficient as $c \doteq re^{i\theta}$, and, since there does not exist a stable fundamental solution of the inverse diffusion process, restrict ourselves to a positive real value of c, that is $\theta\in(-\frac{\pi}{2},\frac{\pi}{2})$. Replacing the real time variable t by a complex time $\tau = ct$, we get $I_\tau = I_{xx}$, $I(x;0)=I_0$. This is the linear diffusion equation with the Gaussian function being its fundamental solution. Reverting back to t, we get:

$$h(x;t) = \frac{K}{2\sqrt{\pi tc}}e^{-x^2/(4tc)}, \tag{9}$$

where $K\in\mathbb{C}$ is a constant calculated according to the initial conditions. For $c\in\mathbb{R}$ we have $K=1$. Separating the real and imaginary exponents we get:

$$\begin{aligned} h(x;t) &= \tfrac{Ke^{-i\theta/2}}{2\sqrt{\pi tr}}e^{-x^2\cos\theta/(4tr)}e^{ix^2\sin\theta/(4tr)} \\ &= KAg_\sigma(x;t)e^{i\alpha(x)}, \\ &\quad \text{where } A=\tfrac{e^{-i\theta/2}}{\sqrt{\cos\theta}}, \quad g_\sigma(x;t)=\tfrac{1}{\sqrt{2\pi}\sigma(t)}e^{-x^2/2\sigma^2(t)}, \end{aligned}$$

and

$$\alpha(x) = \frac{x^2 \sin\theta}{4tr}, \quad \sigma(t) = \sqrt{\frac{2tr}{\cos\theta}}. \tag{10}$$

Satisfying the initial condition $I(x;0) = I_0$ requires

$$h(x; t \to 0) = \delta(x).$$

Since

$$\lim_{t\to 0} g_\sigma(x;t)e^{i\alpha(x)} = \delta(x),$$

we should require $K = 1/A$ (indeed we see that $K = 1$ for the case of positive real c ($\theta = 0$)). The fundamental solution is therefore:

$$h(x;t) = g_\sigma(x;t)e^{i\alpha(x)}, \tag{11}$$

with the Gaussian's standard deviation σ and exponent function $\alpha(x)$ as defined in (10).

2.3 Approximate Solution for Small Theta

We will now show that as $\theta \to 0$ the imaginary part can be regarded as a smoothed second derivative of the initial signal, factored by θ and the time t. Generalizing the solution to any dimension with Cartesian coordinates $\mathbf{x} \doteq (x_1, x_2, ..x_N) \in \mathbb{R}^N$, $I(\mathbf{x};t) \in \mathbb{C}^N$ and denoting that in this coordinate system $\mathbf{g}_\sigma(\mathbf{x};t) \doteq \prod_i^N g_\sigma(x_i;t)$, we show that:

$$\lim_{\theta\to 0} \frac{Im(I)}{\theta} = t\Delta \mathbf{g}_{\tilde{\sigma}} * I_0, \tag{12}$$

where $Im(\cdot)$ denotes the imaginary value and $\tilde{\sigma} = lim_{\theta\to 0}\sigma = \sqrt{2t}$. For convenience we use here a unit complex diffusion coefficient $c = e^{i\theta}$. We use the following approximations for small theta: $cos\theta = 1 + O(\theta^2)$ and $sin\theta = \theta + O(\theta^3)$. Introducing an operator $\tilde{H}$ which is similar to the Schrödinger operator we can write equation (7) (in any dimension) as:

$$I_t = \tilde{H}I, \qquad \text{where } \tilde{H} = c\Delta, \quad I|_{t=0} = I_0. \tag{13}$$

The solution is

$$I = e^{t\tilde{H}}I_0, \tag{14}$$

and is the equivalent of (8), (11). Using the above approximations we get:

$$\begin{aligned} I(\mathbf{x},t) &= e^{ct\Delta}I_0 = e^{e^{i\theta}t\Delta}I_0 \\ &\approx e^{(1+i\theta)t\Delta}I_0 = e^{t\Delta}e^{i\theta t\Delta}I_0 \\ &\approx e^{t\Delta}(1 + i\theta t\Delta)I_0 = (1 + i\theta t\Delta)\mathbf{g}_{\tilde{\sigma}} * I_0. \end{aligned}$$

Note that we used here the identity $e^{t\Delta}X \equiv \mathbf{g}_{\tilde{\sigma}} * X$ that can be proved using the uniqueness of the solution of the diffusion equation or by using the Fourier transform for derivatives $\delta'(x) \leftrightarrow i\omega$.

A thorough analysis of the approximation error with respect to time and θ will be presented elsewhere. We should comment that part of the error depends on the higher order derivatives (4th and higher) of the signal, but, as these derivatives are decaying exponentially by the Gaussian convolution, this error diminishes quickly with time. Numerical experiments show that for $\theta = \pi/30$ the peak error is $\sim 0.1\%$ for the real part and $3-5\%$ for the imaginary part (depending on the signal). Though the peak value error of the imaginary part seems large, the zero crossing location remains essentially accurate.

Some further insight into the behavior of the small theta approximation can be gained by separating real and imaginary parts of the signal and diffusion coefficient in to a set of two equations. Assigning $I = I_R + iI_I$, $c = c_R + ic_I$, we get

$$\begin{cases} I_{Rt} = c_R I_{Rxx} - c_I I_{Ixx} & , I_R|_{t=0} = I_0 \\ I_{It} = c_I I_{Rxx} + c_R I_{Ixx} & , I_I|_{t=0} = 0, \end{cases} \tag{15}$$

where $c_R = \cos\theta$, $c_I = sin\theta$. Assuming that the relation $I_{Rxx} \gg \theta I_{Ixx}$ holds, we can omit the right term of the first equation to get the small theta approximation:

$$\begin{cases} I_{Rt} \approx I_{Rxx} \\ I_{It} \approx I_{Ixx} + \theta I_{Rxx} \end{cases} \tag{16}$$

One can see that the real value part I_R is controlled by a linear forward diffusion equation, whereas the imaginary part I_I is affected by both the real and imaginary equations. We can regard the imaginary part as

$$I_{It} \approx \theta I_{Rxx} + (\text{"a smoothing process"}).$$

2.4 Examples

We present examples of 1D and 2D signal processing with complex diffusion processes characterized by small and large values of θ. In Figs. (1) and (2) a unit step is processed with small and large θ ($\frac{\pi}{30}, \frac{14\pi}{30}$ respectively). In Figs. (3) and (4) the cameraman image is processed with same θ values. The edge detection (smoothed second derivative) qualitative properties are clearly apparent in the imaginary part for the small θ value, whereas the real value depicts the properties of ordinary Gaussian scale-space. For large θ however, the imaginary part feeds back into the real part significantly, creating wave-like structures. In addition, the signal exceeds the original maximum and minimum values, violating the "Maximum-minimum" principal.

3 Nonlinear Complex Diffusion

Nonlinear complex processes can be derived from the above mentioned properties of the linear complex diffusion for purposes of signal and image denoising or enhancement. We suggest an example of a nonlinear process for ramp edges denoising purposes (different from the widely used step edges denoising methods).

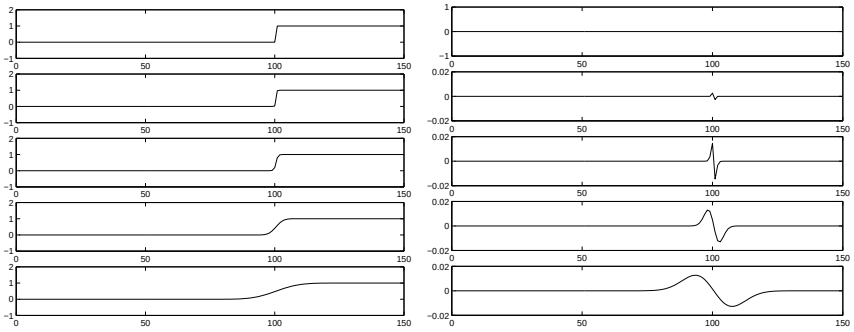

Fig. 1. Complex diffusion of a small theta applied to a step signal ($\theta = \pi/30$). Left - real values, right - imaginary values. Each frame depicts from top to bottom: original step, diffused signal after times: 0.025, 0.25, 2.5, 25.

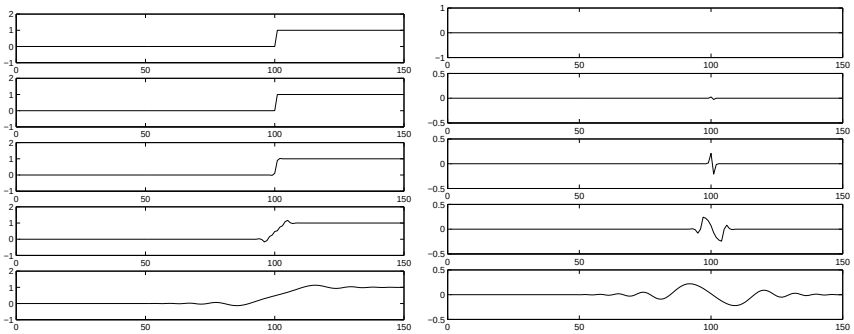

Fig. 2. Complex diffusion of a large theta applied to a step signal ($\theta = 14\pi/30$). Top - real values, bottom - imaginary values. Each frame depicts from top to bottom: original step, diffused signal after times: 0.025, 0.25, 2.5, 25.

We define the following 1D unit ramp:

$$R(x) = \begin{cases} 0 \ , x < 0 \\ x \ , 0 \leq x \leq 1 \\ 1 \ , x > 1 \end{cases} \tag{17}$$

We are looking for a general nonlinear diffusion equation

$$I_t = \frac{\partial}{\partial x} \left(c(\cdot) I_x \right) \tag{18}$$

that preserves smoothed ramps $R(x) * f(x)$, where $f(x)$ is a smoothing kernel. Following the same logic that utilized a gradient measure in order to slow the diffusion near step edges, we search for a suitable differential operator $\mathcal{D}$ for ramp

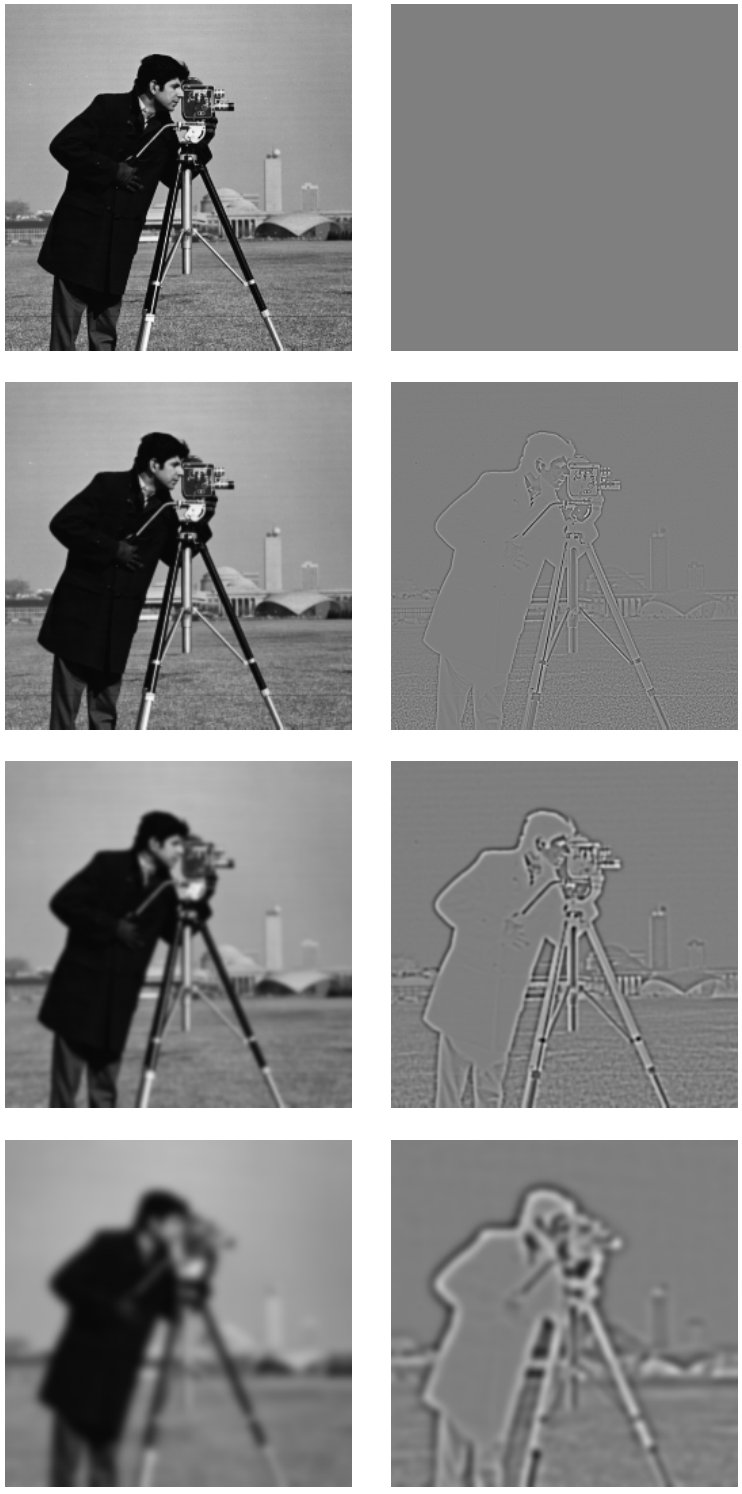

Fig. 3. Complex diffusion of the cameraman image for small theta ($\theta = \pi/30$). Left - real values, right - imaginary values (factored by 20). Each frame (from top to bottom): original, image after times: 0.025, 0.25, 2.5, 25.

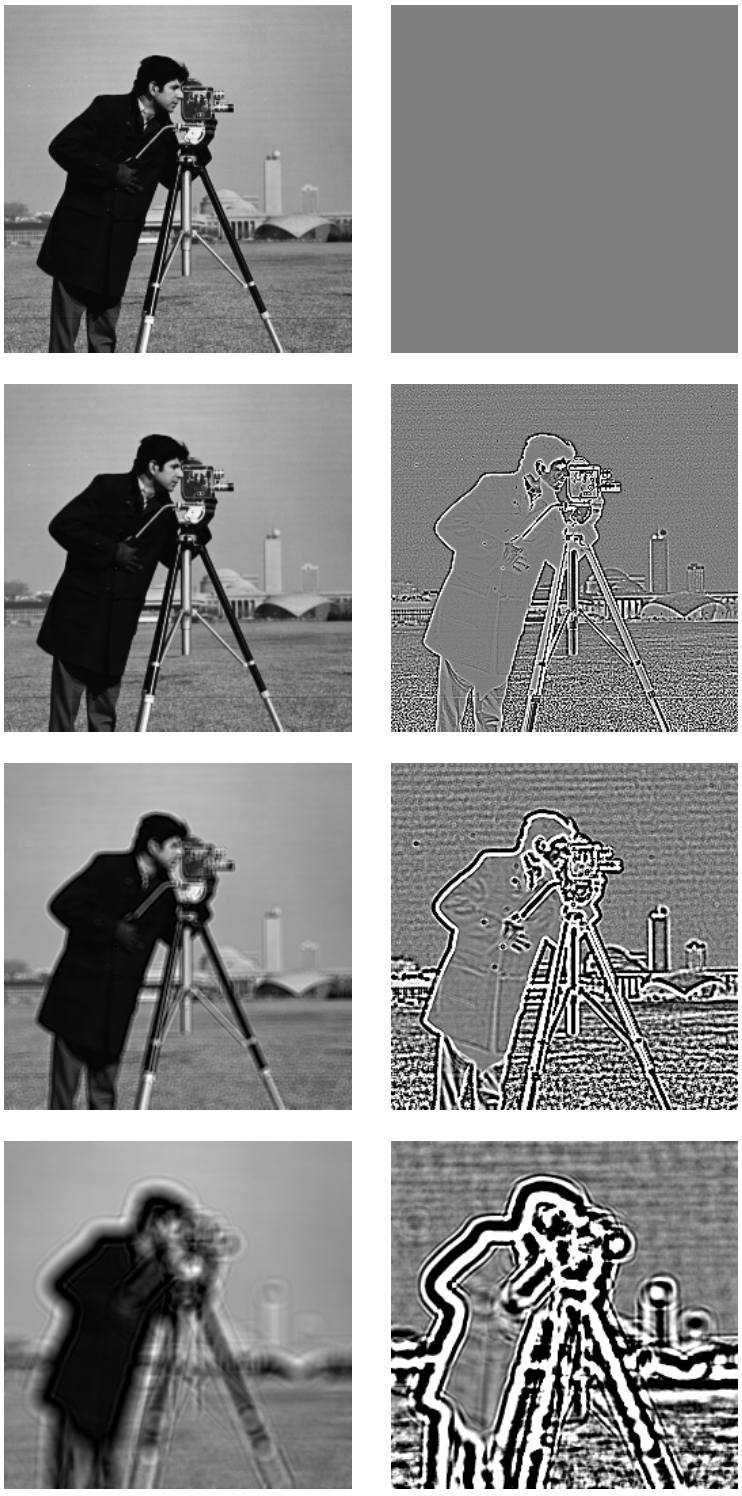

Fig. 4. Complex diffusion of the cameraman image for large theta ($\theta = 14\pi/30$). Left - real values, right - imaginary values (factored by 20). Each frame (from top to bottom): original, image after times: 0.025, 0.25, 2.5, 25.

edges. Eq. (18) with a diffusion coefficient $c(|\mathcal{D}I|)$ which is a decreasing function of $|\mathcal{D}I|$ can be regarded as a ramp preserving process. We begin by examining the gradient, as a possible candidate, concluding that it is not a suitable measure for two reasons: The gradient does not detect the ramp main features - namely its endpoints; Moreover, it has a nearly uniform value across the whole smoothed ramp, causing a nonlinear gradient-dependent diffusion to slow the diffusion process in that region, thus not being able to properly reduce noise within a ramp (creating staircasing effects). The second derivative (Laplacian in multiple dimensions) is a suitable choice: It has a high magnitude near the endpoints and low magnitude everywhere else - and thus enables the nonlinear diffusion process to reduce noise within a ramp. Note that a ramp can be regarded as an integration of two steps with opposite signs, and therefore it makes sense to take a second derivative as a simple ramp detector (compared to a first derivative for a step detector).

We formulate $c(s)$ as a decreasing function of s:

$$c(s) = \frac{1}{1+s^2}, \text{ where } c(s) = c(I_{xx}). \tag{19}$$

Using the c of (19) in (18) we get:

$$I_t = \frac{\partial}{\partial x}\left(\frac{I_x}{1+I_{xx}^2}\right) = \frac{1+I_{xx}^2-2I_xI_{xxx}}{(1+I_{xx}^2)^2}I_{xx}. \tag{20}$$

There are two main problems in this scheme. The first and more important one is the fact that noise has very large (theoretically unbounded) second derivatives. Secondly, a numerical problem arises as third derivatives should be computed, with large numerical support and noisier derivative estimations. These two problems are solved by using the nonlinear complex diffusion.

Following the results of the linear complex diffusion (Eq. 12) we estimate by the imaginary value of the signal divided by θ, the smoothed second derivative multiplied by the time t.

Whereas for small t this terms vanish, allowing stronger diffusion to reduce the noise, with time its influence increases preserving the ramp features of the signal. We should comment that these second derivative estimations are more biased than in the linear case, as we have a nonlinear process.

The equation for the multidimensional process is

$$\begin{aligned} I_t &= \nabla \cdot (c(Im(I))\nabla I), \\ c(Im(I)) &= \frac{e^{i\theta}}{1+\left(\frac{Im(I)}{k\theta}\right)^2}, \end{aligned} \tag{21}$$

where k is a threshold parameter. The phase angle θ should be small ($\theta << 1$). Since the imaginary part is normalized by θ, the process is not affected much by changing the value of θ as long as it stays small.

We implement this flow with forward Euler scheme with central difference approximation for the spatial derivatives and backward time derivative. Care

should be exercised when choosing the time step. The fundamental solution includes a Gaussian with variance $\sigma^2 = \frac{2tr}{\cos\theta}$. Implementing Gaussian convolution of time τ by incremental time steps where $\sigma^2 = 2\tau$ requires the time step bound to be: $\Delta\tau \leq 0.25h^2$ (in 2 dimensions, where h is the spatial step). Here we have $\tau = \frac{tr}{\cos\theta}$ and hence in the general case we require: $\Delta t \leq 0.25h^2\frac{\cos\theta}{r}$, and for our case where r=1, h=1: $\Delta t \leq 0.25\cos\theta$.

This means that when θ approaches $\pi/2$ it is very inefficient to implement complex diffusion with incremental time-steps. For small θ there is essentially no difference than real diffusion (works also in the nonlinear case).

In Figs. 5, 6 and 7 we show an example of a noisy ramp denoised by the P-M process in comparison to the above process (with $\theta = \frac{\pi}{30}$). One can notice that the known P-M's staircasing effect does not happen in our nonlinear complex scheme. In Fig. 8 the process is applied to an apple image that contains both sharp (step) and gradual (ramp) edges.

4 Conclusion

The fundamental solution for the linear complex diffusion indicates that there exists a stable process for $\theta \in (-\frac{\pi}{2}, \frac{\pi}{2})$. In the case of small θ two observations are relevant to the application of the complex diffusion process in image processing: The real function equation is effectively decoupled from the imaginary one, and behaves like a real linear diffusion process; The imaginary part is approximately a smoothed second derivative of the real part. Therefore, we can regard the Gaussian and Laplacian "pyramids" (scale-spaces) as results of a single complex diffusion equation.

Although the nonlinear scheme remains to be better analyzed and understood, a ramp preserving denoising process was demonstrated as an example of possible applications of complex diffusion schemes.

Acknowledgments

This research has been supported in part by the Ollendorf Minerva Center, by the Fund for the Promotion of Research at the Technion, by the Israeli Ministry science, and by the Technion V.P.R. Fund.

References

1. J.J. Koenderink, "The structure of images", *Biol. Cybern.*, 50: 363-370, 1984.
2. M. Nagasawa, *S*hrödinger equations and diffusion theory, Monographs in mathematics, vol. 86, Birkhäuser Verlag, Basel, Switzerland 1993.
3. P. Perona and J. Malik, "Scale-space and edge detection using anisotropic diffusion", IEEE Trans. Pat. Anal. Machine Intel., vol. PAMI-12,no. 7, pp. 629-639, 1990.
4. B M ter Haar Romeny Ed., *G*eometry Driven Diffusion in Computer Vision, Kluwer Academic Publishers, 1994.
5. A. P. Witkin, "Scale space filtering", Proc. Int. Joint Conf. On Artificial Intelligence, pp. 1019-1023, 1983.

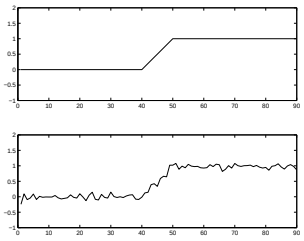

Fig. 5. Original (top) and noisy (bottom) ramp signal.

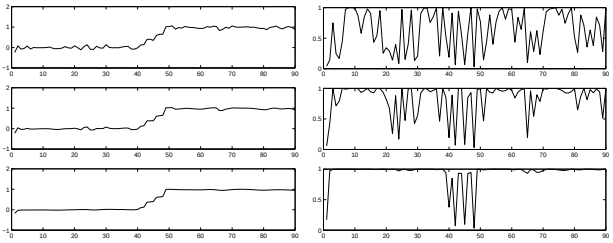

Fig. 6. Perona-Malik nonlinear diffusion of a ramp edge ($k = 0.1$). Left - signal, right - value of c. Each frame from top to bottom is for the signal after time: 0.25, 1, 2.5.

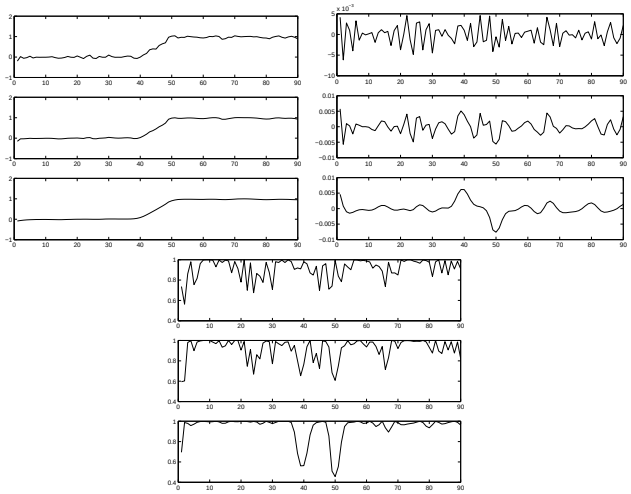

Fig. 7. Nonlinear complex diffusion of a ramp edge ($\theta = \pi/30$, $k = 0.07$). Left - real values, right - imaginary values, bottom - real value of c. Each frame from top to bottom is for the signal after time: 0.25, 1, 2.5.

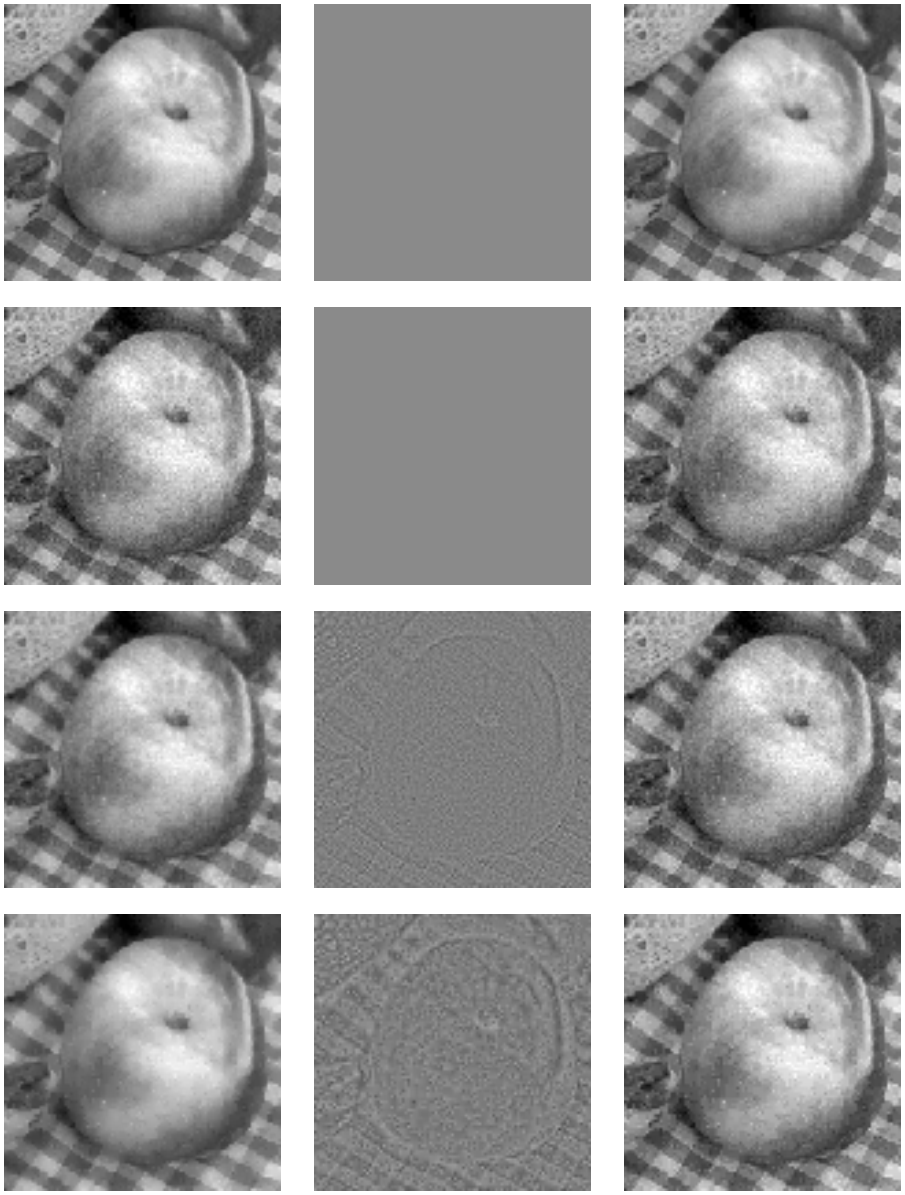

Fig. 8. Nonlinear diffusion of an apple image: Right row - complex nonlinear scheme ($\theta = \pi/30$, $k = 2$) real part, middle row - imaginary part, left row - Perona-Malik ($k = 3$). In each row, frames from top to bottom: original image, image corrupted by white Gaussian noise, image after times: 0.25, 2.5. One can see that the apple is better denoised in the complex scheme, where staircasing effects appear in the P-M process. The map (step edges), on the other hand, is better preserved by the P-M process. Trying to increase the P-M threshold in order to avoid staircasing causes the whole apple to get diffused with the background. Another observation is that the complex scheme denoises faster (due to its implicit time dependency).